Supplementary information for

A low-dimensional N-rich coordination polymer as effective fluorescence sensor for 2,4,6-trinitrophenol detection in an aqueous medium

Xu Han,[a] Jialin Tong,[b] Guanyu Ding,[a] Chunyi Sun,[b] Xinlong Wang,[b] Zhongmin Su,[*a] Jing Sun,[a] Li-Li Wen,[*a] Guo-Gang Shan[*b]

[a]School of Chemical and Environmental Engineering, Changchun University of Science and Technology, Changchun, 130022, PR China.

E-mail: zmsu@nenu.edu.cn, wll@cust.edu.cn

[b]National & Local United Engineering Laboratory for Power Batteries, Key Laboratory of Polyoxometalate Science of Ministry of Education, Department of Chemistry, Northeast Normal University, Changchun 130024, China.

E-mail: shangg187@nenu.edu.cn

Caption of Figure

Caption of Table

Experimental section

1.1 Materials

Anhydrous $InCl_3$ and all the nitroaromatics were obtained from Sinopharm Chemical Reagent *Co., Ltd*. China. 4-(tetrazol-5-yl) phenyl-[2,2′:6′,2″]terpyridine) (HTzPTpy) for the synthesis were purchased from Tensus Biotech (Shanghai) Co. The purity of all reagents was of analytical grade and was used without further purification. Aqueous solutions were prepared with deionized water (18.2 MΩ cm) produced from a Milli-Q water purification system.

Caution! 2,4,6-trinitrophenol (TNP) possesses highly explosive and should be handled carefully and in small amounts.

1.2 Characterization

Powder X-ray diffraction (PXRD) patterns of the samples were recorded ranging from 5 to 50° at room temperature using a Siemens D5005 X-ray diffractometer with Cu-Kα radiation (λ = 1.5418 Å). The FTIR spectrum was performed in the range of 4000-400 cm^{-1} using KBr pellets on an Alpha Centauri FTIR spectrophotometer. The UV-Visible absorption spectra were obtained with a Shimadzu UV-3900 spectrophotometer. Thermogravimetry analysis (TGA) was performed on a Mettler Toledo DTG-60H System apparatus under Nitrogen flow (50 mL min^{-1}) at a heating rate of 5 °C min^{-1} up to 800 °C. Photoluminescence (PL) spectra are scanned on a photoluminescence spectrometer (Hitachi F-4600) under an excitation wavelength of 360 nm. Lifetime measurements were performed on Edinburgh Fluorescence Spectrometer (FLS920P).

X-ray single-crystal data collection of **CUST-801** was performed on a Bruker APEX II CCD diffractometer equipped with a graphite monochromator using Mo-Ka radiation (λ=0.71073 Å) at 245 K. A multiclan technique was applied to perform adsorption corrections. The structures were solved using the direct method and refined using the full-matrix least-squares method on F2 with anisotropic thermal parameters for all non-hydrogen atoms using the SHELXL-2014 program.[1-3] The crystallographic

data of **CUST-801** have been deposited in the Cambridge Crystallographic Data Center with CCDC 2115226.

Fluorescence experiments

In the typical experimental setup, 3 mg of **CUST-801** was dispersed in 10 mL of deionized water. In a 1 cm quartz cuvette, 3 mL solution of **CUST-801** (0.9 mg/mL) was placed and the fluorescence response was measured in-situ after incremental addition of freshly prepared analyte solutions. The fluorescence response was measured in the range of 400-750 nm upon excitation at 380 nm while keeping a 5 nm slit width for both source and detector. To maintain homogeneity, the sample was sonicated and ground during the experiment.

Formula for calculating the percentage of TNP fluorescence intensity quenching:[4, 5]

$$\frac{Io - I}{Io} \times 100\%$$

Where, I_0 = initial fluorescence intensity,

I = intensity of **CUST-801** containing TNP solution.

Stern-Volmer equation:[6]

$$I0/I = KSV[M] + 1$$

Where, I_0 = fluorescent intensity of **CUST-801** before the addition of the analyte,

I = fluorescent intensity after the addition of the respective analyte,

K_{SV} = Stern-Volmer constant,

[M] = molar concentration of the analyte (M^{-1}).

The limit of detection concentration (LOD) was calculated according to the formula:[7]

$$LOD = 3\delta/K_{SV}$$

δ is the standard deviation of the detection method.

Table S1. Crystal data and structure refinement for **CUST-801**

CCDC	2115226
Empirical formula	$C_{22}H_{14}Cl_2InN_7$
Formula weight	562.12
Temperature /K	244.64
Crystal system	monoclinic
Space group	$P2_1/n$
a /Å	9.1353(15)
b /Å	19.683(3)
c /Å	11.535(2)
α /°	90
β /°	93.588(7)
γ /°	90
Volume/Å^3	2070.0 (6)
Z	4
ρ_{calc}g/cm^3	1.804
Radiation	Mo Kα (λ = 0.71073)
Independent reflections	3661 [R_{int}= 0.0409, R_{sigma}= 0.0219]
2θ range for data /°	4.924 to 50.174
Goodness-of-fit on F^2	1.259
Final R indexes [I>=2σ (I)]	0.0242
Final R indexes [all data]	0.0799

$^aR_1 = \sum||F_o| - |F_c|| / \sum|F_o|$. $^bwR_2 = \{[\sum w (F_o^2 - Fc^2)^2]/\sum[w(F_o^2)^2]\}^{1/2}$

Table S2. Bond Lengths for **CUST-801**

Atom	Atom	Length
In1	Cl1	2.4618 (11)
In1	Cl2	2.4038 (9)
In1	N1	2.236 (2)
In1	N2	2.265 (2)
In1	N3[1]	2.297 (3)
In1	N4	2.292 (3)
In1[2]	N3	2.297 (3)
C1	C4	1.495 (4)
N6	N7	1.362 (4)

[1]3/2-X,-1/2+Y,3/2-Z,[2]3/2-X,1/2+Y,3/2-Z

Table S3. Bond Angles for CUST-801

Atom	Atom	Atom	Angle	Atom	Atom	Atom	Angle
Cl2	In1	Cl1	92.71 (4)	N2	In1	N4	143.98 (9)
N1	In1	Cl1	92.13 (7)	N3[1]	In1	Cl1	173.70 (6)
N1	In1	Cl2	174.08 (7)	N3[1]	In1	Cl2	93.45 (7)
N1	In1	N2	71.99 (8)	N4	In1	Cl1	90.56 (8)
N1	In1	N3[1]	81.81 (9)	N4	In1	Cl2	111.34 (7)
N1	In1	N4	72.02 (9)	N3[1]	In1	N4	85.97 (10)
N2	In1	Cl1	92.14 (7)	C1	N1	In1	119.31 (18)
N2	In1	Cl2	104.40 (7)	C1	N1	C7	120.9 (2)
N2	In1	N3[1]	87.61 (9)	C7	N1	In1	119.73 (19)
C4	N2	In1	117.64 (19)	C12	N4	In1	116.57 (19)
N5	N3	In1[2]	113.8 (2)	C20	N4	In1	124.6 (2)
C18	N3	In1[2]	135.9 (2)	C3	C1	C4	124.2 (3)

[1]3/2-X,-1/2+Y,3/2-Z; [2]3/2-X,1/2+Y,3/2-Z

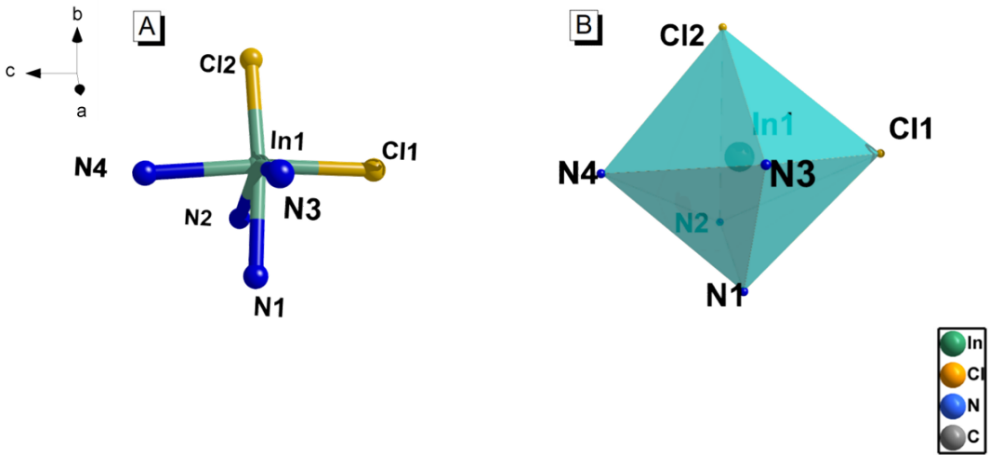

Figure S1. Co-ordination environment around the In (III) center. Color code: Indium (sea green), Chlorine (light orange), Nitrogen (blue), Carbon (grey). (Hydrogen atoms are omitted for clarity).

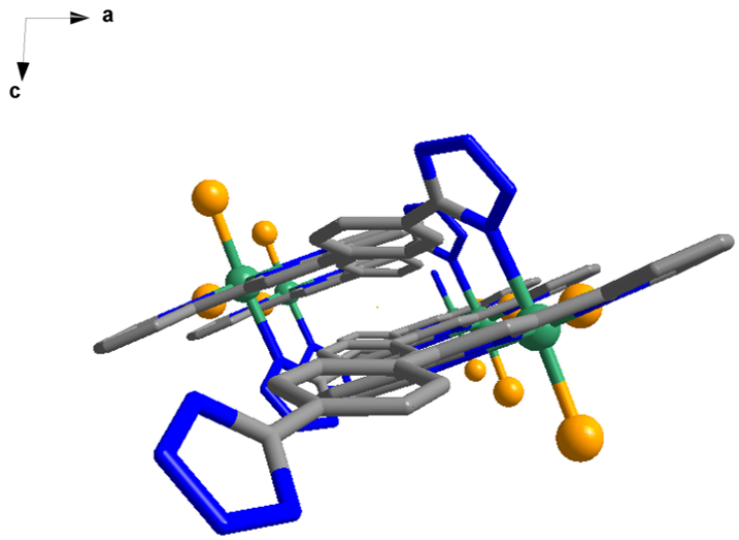

Figure S2. View of the b axis. Color code: same as Figure S1.

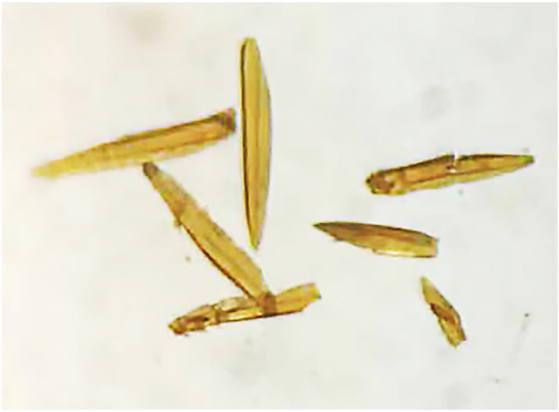

Figure S3. Visible images of **CUST-801** crystals.

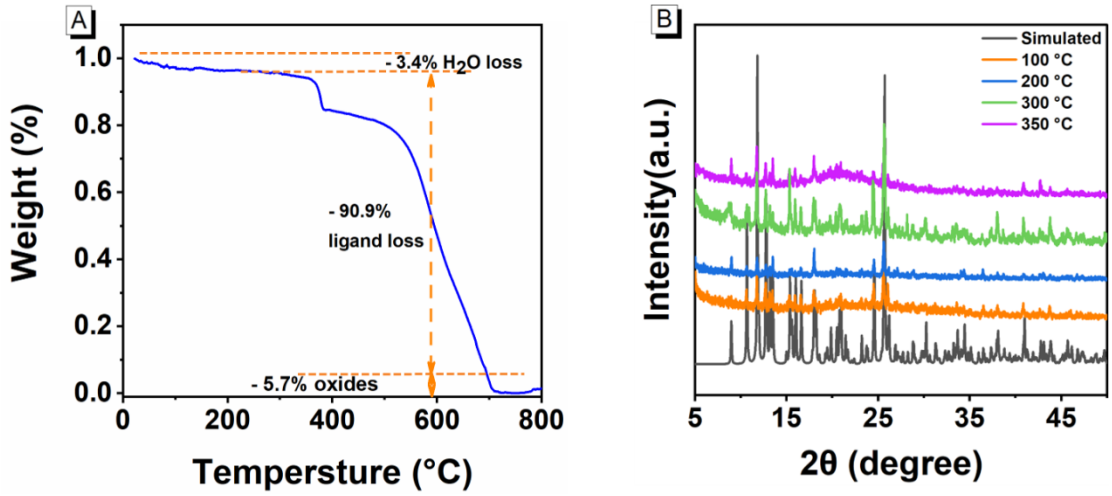

Figure S4. (A) Thermogravimetric analysis curve of **CUST-801**. (B) Simulated and experimental powder X-ray diffraction patterns (PXRD) patterns of **CUST-801** are heated at 200 ℃, 300 ℃, 350 ℃.

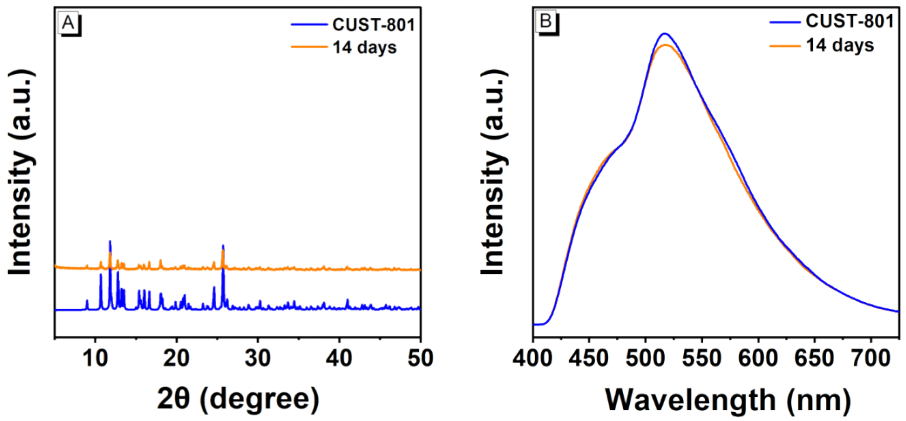

Figure S5. (A) Powder X-ray diffraction pattern of **CUST-801** in 14 days with water. (B) Luminescence spectrum of **CUST-801** and after storage in water for 14 days.

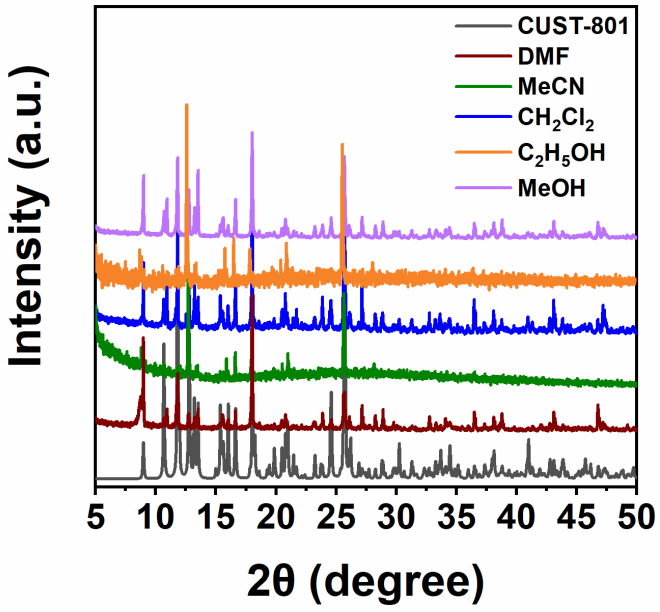

Figure S6. Powder X-ray diffraction patterns of **CUST-801** in different organic solvents.

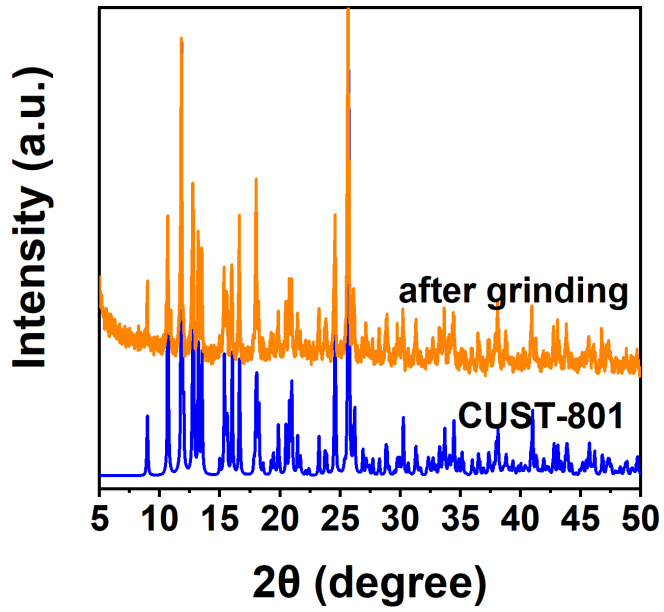

Figure S7. Powder X-ray diffraction patterns of **CUST-801** after grinding.

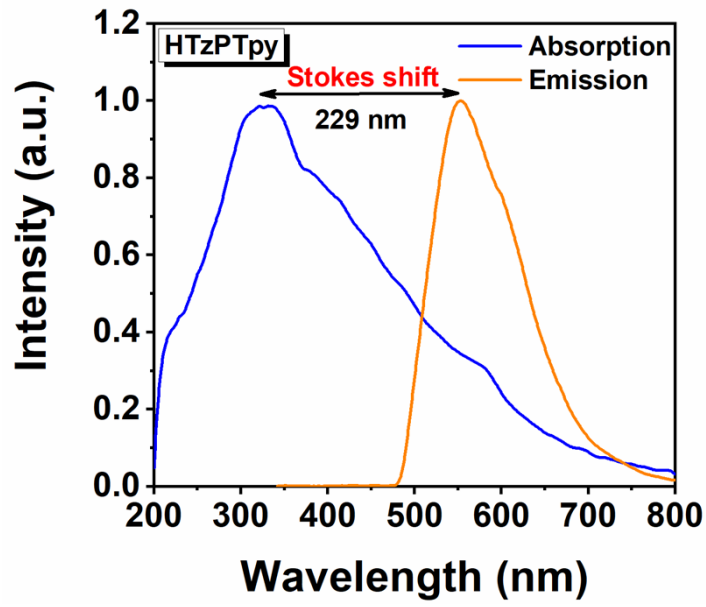

Figure S8. The solid-state excitation and emission spectra of free HTzPTpy ligand. (λ_{ex} = 324 nm; λ_{em} = 553 nm).

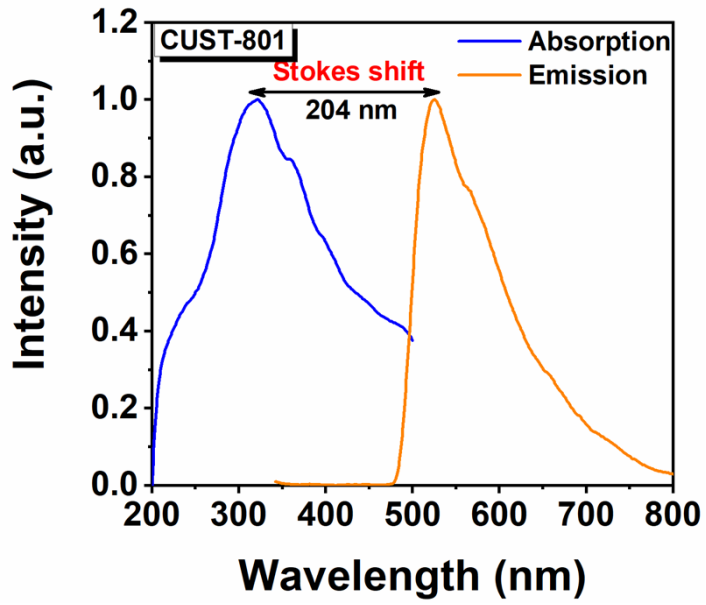

Figure S9. The solid-state excitation and emission spectra of **CUST-801**. (λ_{ex} = 320 nm; λ_{em} = 524 nm).

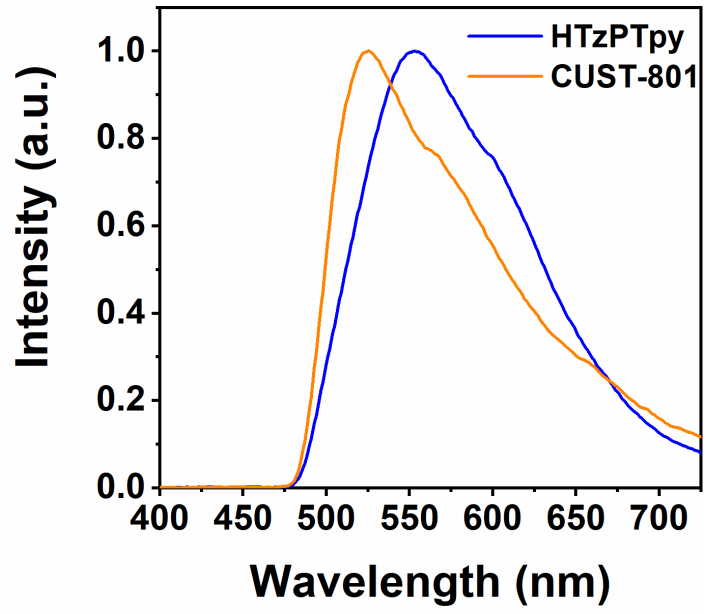

Figure S10. The solid-state peak of fluorescence emission of free **HTzPTpy** ligand and **CUST-801** (λ_{ex} = 320 nm).

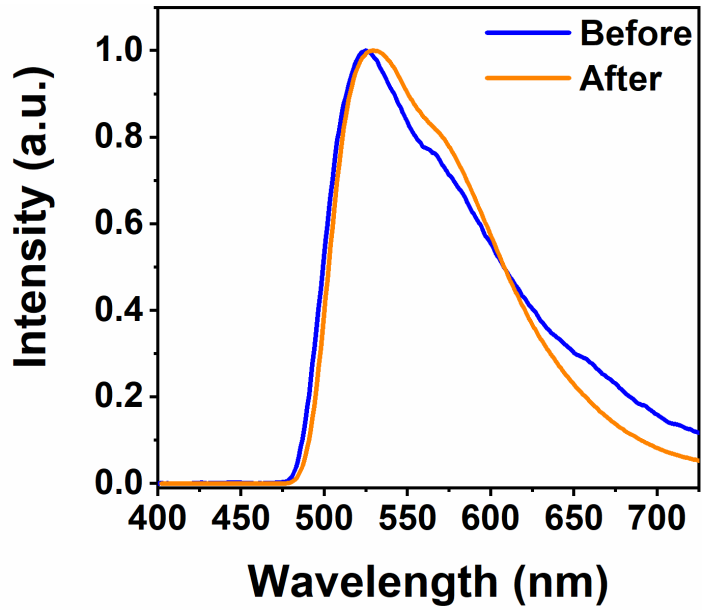

Figure S11. The solid-state peak position of the emission fluorescence spectrum of **CUST-801** after grinding treatment (λ_{ex} = 320 nm).

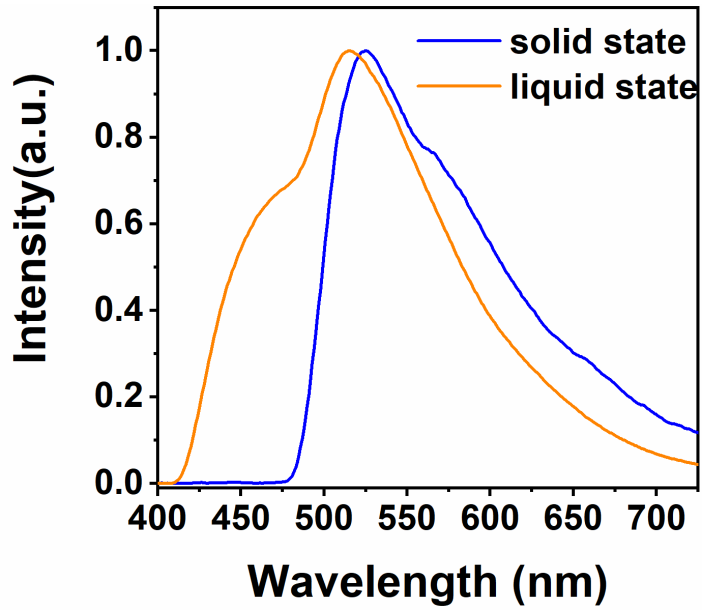

Figure S12. The solid-state and the liquid-state peak of fluorescence emission for **CUST-801** (solid: λ_{ex}= 320 nm, liquid: λ_{ex}= 380 nm).

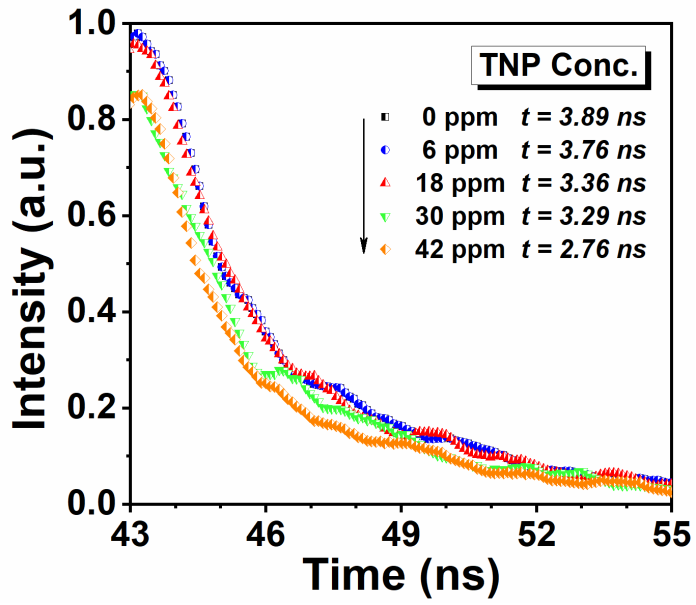

Figure S13. Lifetime decay profiles of **CUST-801** in water containing different amounts of TNP (from 0 to 42 ppm).

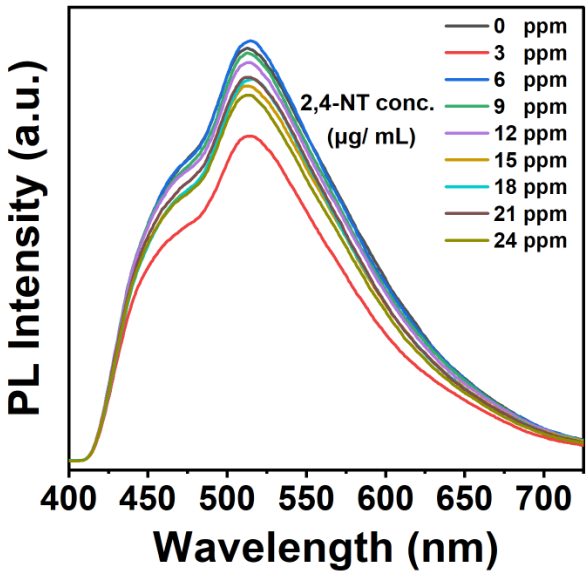

Figure S14. Photoluminescence spectra of **CUST-801** in water containing different amounts of 2,4-NT (λ_{ex}= 380 nm).

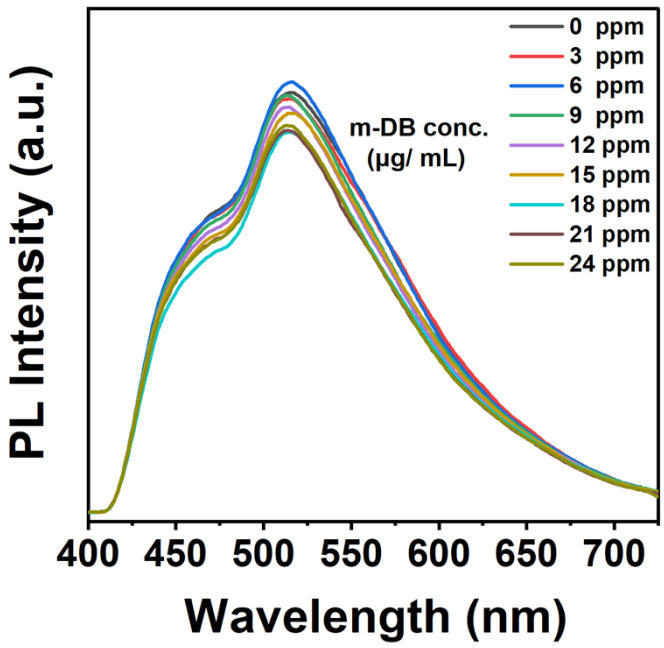

Figure S15. Photoluminescence spectra of **CUST-801** in water containing different amounts of m-DB (λ_{ex} = 380 nm).

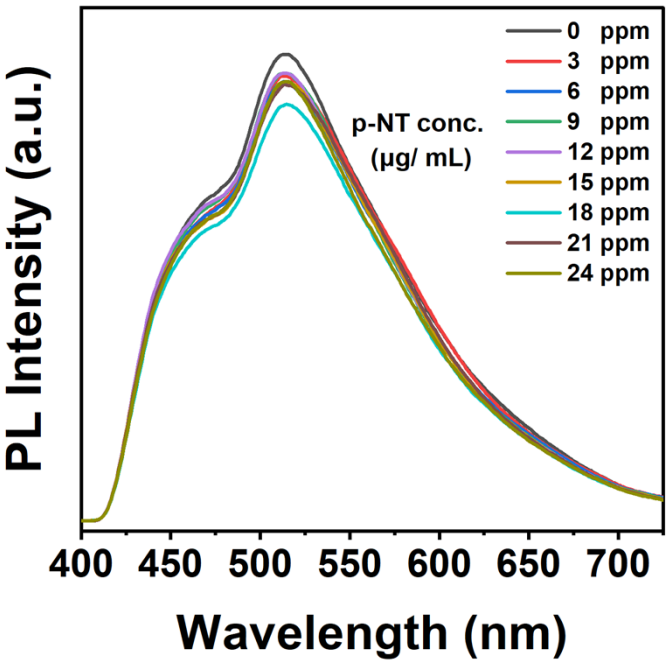

Figure S16. Photoluminescence spectra of **CUST-801** in water containing different amounts of p-NT (λ_{ex} = 380 nm).

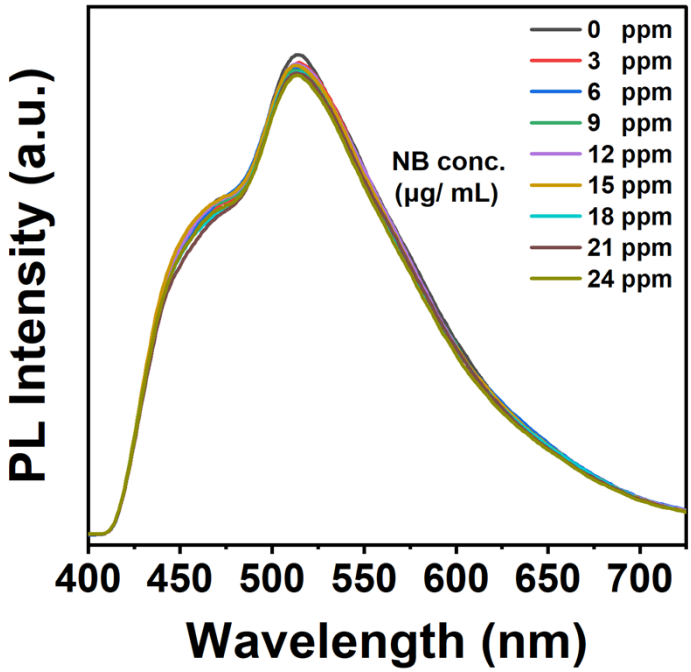

Figure S17. Photoluminescence spectra of **CUST-801** in water containing different amounts of NB (λ_{ex} = 380 nm).

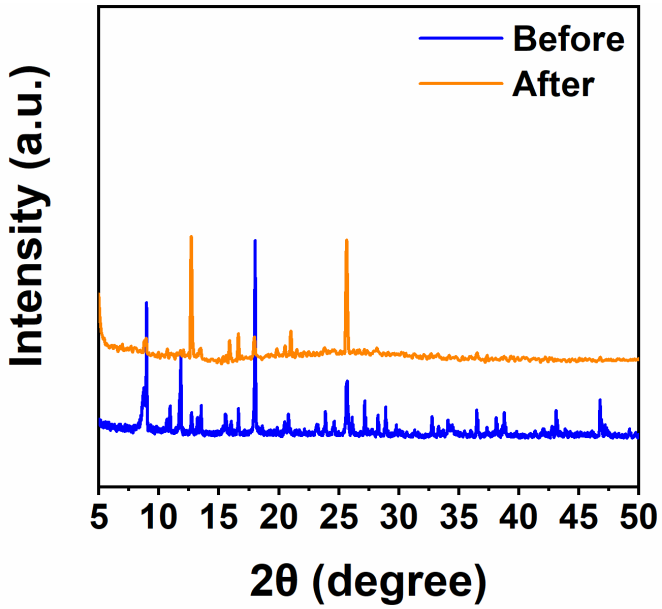

Figure S18. Powder X-ray diffraction pattern of **CUST-801** after recycling.

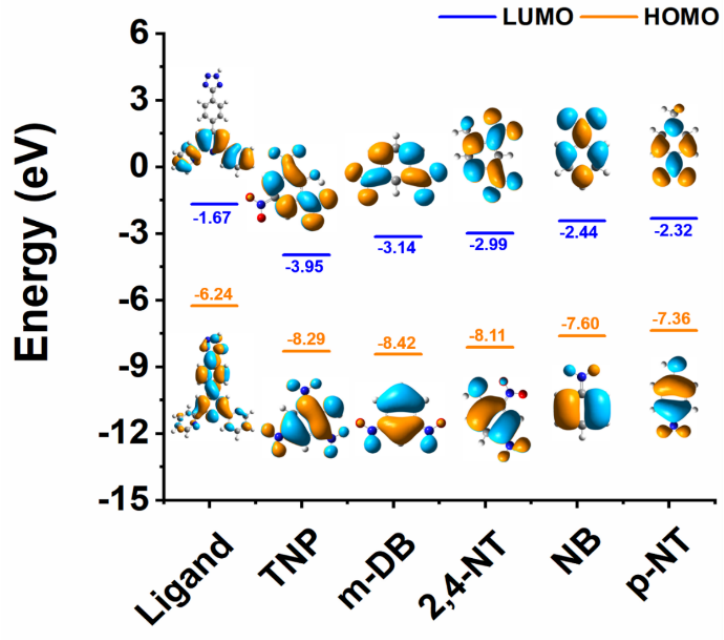

Figure S19. LUMO and HOMO energy of NACs and ligands.

Table S4. The comparison of the quenching constants (K_{SV}) and the detection limit with reported CPs for sensing TNP.

Molecular Formula	(K_{SV}/M^{-1})	Detection Limit	solvent	Ref.
CUST-801	8.95×10^4	1.34 μM (0.3 ppm)	Water	**This work**
$(CH_3)_2NH_2][Cd(1245\text{-}BTC)_{0.5}(3S\text{-}TRZ)$	1.0×10^4	23.6 μM	DMF	[8]
$[Zn_2(tpbn)(2,6\text{-}NDC)_2]n$	5.907×10^3	47.54 μM	water	[9]
$[[Zn_2(tphn)(2,6\text{-}NDC)_2]\cdot4H_2O]n$	2.464×10^3	82.11 μM	water	[9]
$[ZnL1(2,6\text{-}BIP)]\cdot2H_2O\cdot DMF$	1.48×10^4	4.05 μM (0.84 ppm)	DMF	[10]
$[CdL1(2,6\text{-}BIP)]\cdot2H_2O\cdot DMF$	1.44×10^4	3.94 μM	DMF	[10]
$[Zn_2L2(2,6\text{-}BIP)]\cdot DMF$	5×10^4	1.16 μM (260 ppb)	DMF	[10]
$[CdL2(2,6\text{-}BIP)]\cdot DMF$	5.31×10^4	1.1 μM	DMF	[10]
$[Zr_6O_4(OH)_4(BTDB)_6]\cdot8H_2O\cdot6DMF$	2.49×10^4	1.63 μM	MeOH	[11]
$[Cd(INA)(pytpy)(OH)\cdot2H_2O]n$	3.3×10^4	9.1 μM	water	[12]
$Zn_2(H_2L)_2(Bpy)2(H_2O)3\cdot H_2O$	1.36×10^4	0.49 μM	water	[13]
$[Zn(L)(HCOO)\cdot H_2O]n$	2.11×10^4	-	water	[14]
$[Zn_4(DMF)(Ur)_2(NDC)_4]n$	1.083×10^5	7.1 μM	water	[15]
$Zr_6O_4(OH)_4(L)_6$	2.9×10^4	2.6 μM	water	[16]
$[Eu_3(bpydb)_3(HCOO)(\mu_3\text{-}OH)_2(H)]$	2.1×10^4	-	water	[17]

Some probe for adsorption and detection in water or wastewater

Probes	Analytes	solvent	Ref.
CUST-801	TNP	water	**This work**
SiO2-HMBA	Ce	wastewater	[18]
AcDB20C6	Cs	water	[19]
Ni-Si-MgO/CNTs	H_2	water	[20]
-	Ni	water	[21]
Bio-slag	Cs	wasterwater	[22]

Table S5. HOMO and LUMO energy levels of selected NACs and ligand.

Analytes	HOMO (eV)	LUMO (eV)	Band gap (eV)
TNP	-8.288593	-3.951448	4.337145
2,4-NT	-8.112495	-2.989093	5.123402
m-DB	-8.41705	-3.140347	5.276703
NB	-7.600974	-2.436778	5.164196
p-NT	-7.362160	-2.320531	5.041628

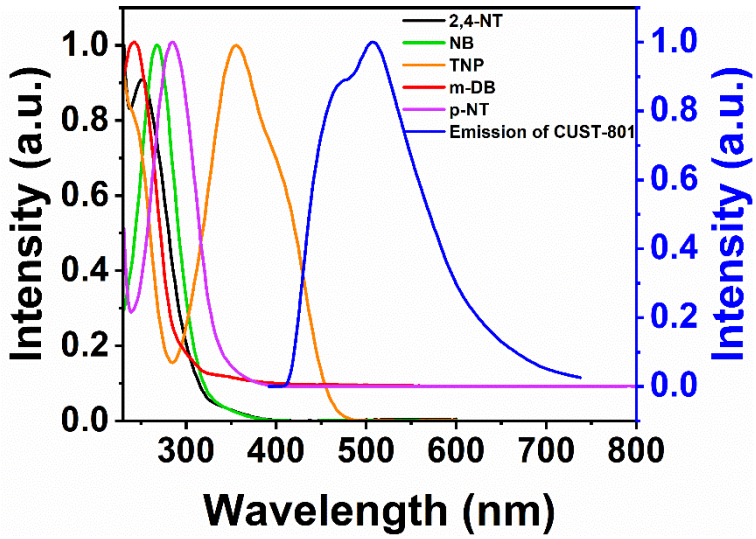

Figure S20. The absorption spectra of difference NACs and emission spectra of **CUST-801**.

References

1. Y. Gong, C. Qin, Y. T. Zhang, C. Y. Sun, Q. H. Pan, X. L. Wang and Z. M. Su, *Angew. Chem. Int. Ed.*, 2020, **59**, 22034-22038.
2. H. M. Gan, N. Xu, C. Qin, C. Y. Sun, X. L. Wang and Z. M. Su, *Nat. Comm.*, 2020, **11**, 1-8.
3. a) G. M. Sheldrick, *Acta Crystallogr. A*, 2008, **64**, 112. b) G. M. Sheldrick, *Acta Crystallogr. C*, 2015, **71**, 3-8.
4. X. G. Hou, W. Yong, H. T. Cao, H. Z. Sun, H. B. Li, G. G. Shan and Z. M. Su, *Chem. Comm.*, 2014, **50**, 6031-6034.
5. Ming Y, Hai H, Peng F, Z. M. Su, X. Li, X. L. Hu, F. W. Gao and Q. Q. Pan. *Dyes Pigm.*, 2020, **185**. 1008825-10088434.
6. S. S. Nagarkar, B. Joarder, A. K. Chaudhari, S. Mukherjee and S. K. Ghosh, *Angew. Chem., Int. Ed.*, 2013, **52**, 2881-2885.
7. W. L. Che, G. F. Li, X. M. Liu, K. Z. Shao, D. X. Zhu, Z. M. Su and M. R. Bryce, *Chem. Commun.*, 2018, **54**, 1730-1733.
8. H. T. Wu, H. P. Li, S. N. Li, Y. C. Jiang, M. C. Hu and Q. G. Zhai, *J. Solid State Chem.*, 2020, **283**, 121166-121174.
9. G. Chakraborty and S. K. Mandal, *Inorg. Chem.*, 2017, **56**, 14556-14566.
10. D. Wang, Z. Y. Hu, S. S. Xu, D. D. Li, Q. Zhang, W. Ma, H. P. Zhou, J. Y. Wu and Y. P. Tian, *Dalton Trans.*, 2019, **48**, 1900-1905.
11. S. K. Mostakim and S. Biswas, *Cryst. Eng. Comm.*, 2016, **18**, 3104-3113.
12. J. F. Zhang, J. J. Wu, G. D. Tang, J. Y. Feng, F. M. Luo, B. Xu and C. Zhang, *Sens. Actuators B Chem.*, 2018, **272**, 166-174.
13. Y. J. Deng, N. J. Chen, Q. Y. Li, X. J. Wu, X. L. Huang, Z. H. Lin and Y. G. Zhao, *Cryst. Growth Des.*, 2017, **17**, 3170-3177.
14. Y. Yang, K. Shen, J. Z. Lin, Y. Zhou, Q. Y. Liu, C. Hang, H. N. Abdelhamid, Z. Q. Zhang and H. Chen, *RSC Adv.*, 2016, **6**, 45475-45481.
15. S. Mukherjee, A. V. Desai, B. Manna, A. I. Inamdar and S. K. Ghosh, *Cryst. Growth Des.,* 2015, **15**, 4627-4634.

16. S. S. Nagarkar, A. V. Desai and S. K. Ghosh, *Chem. Commun.*, 2014, **50**, 8915-8918.
17. X. Z. Song, S. Y. Song, S. N. Zhao, Z. M. Hao, M. Zhu, X. Meng, L. L. Wu and H. J. Zhang, *Adv. Funct. Mater.*, 2014, **24**, 4034-4041.
18. K. T. Kubra, M. S. Salman, M. N. Hasan, A. Islam, S. H. Teo, M. M. Hasan, M. C. Sheikh and M. R. Awual, *J. M. Liq.*, 2021, 338, 116667-116677.
19. M. R. Awual, T. Yaita, T. Kobayashi, H. Shiwaku and S. Suzuki, *J. Environ. Chem. Eng*., 2020, 8, 103684-103693.
20. A. Islam, S. H. Teo, M. R. Awual, Y. Hin and T. Yap, *J. Clean. Prod.*, 2019, 238, 117887-117897.
21. M. A. Islam, M. R. Awual and M. J. Angove, *J. Environ. Chem. Eng.*, 2019, 7, 103305-103321.
22. S. Khandaker, Y. Toyohara, G. C. Saha, M. R. Awual and T. Kuba, *J. WaterProcess Eng.*, 2020, 33, 101055-101064.